Study of πN and KN Elastic and Inelastic Scatterings and Their Polarizations by a Multiple-Regge-Pole Model*

FEI S. CHEN-CHEUNG
Physics Department, St John's University, Jamaica, New York 11432

AND

TIMOTHY ROTH
Physics Department, Carnegie-Mellon University, Pittsburgh, Pennsylvania 15213

(Received 12 May 1967; revised manuscript received 25 March 1968)

The presently available data on pion-nucleon scattering for incident momenta from 6 to 18 GeV/c and for small values of momentum transfer $[|t|<1$ (GeV/c)$^2]$ are analyzed using a model characterized by the dominance of several meson Regge poles in the crossed channels. Among the processes considered are π^+p and π^-p elastic scattering and the charge-exchange reactions $\pi^-p\to\pi^0n$ and $\pi^-p\to\eta^0n$. All the contributing meson trajectories, P, P', ρ, and A_2, are taken into account. The following KN reactions: K^-p, K^-n, K^+p, K^+n elastic scattering and the $K^-p\to K^0n$ charge-exchange reaction, are also analyzed with the contributing trajectories P, P', ρ, A_2, and ω. We find that both σ_{tot} and $d\sigma/dt$ data for pion-nucleon reactions can be very well fitted by the model with energy-independent residue functions. The polarization data are well fitted, and determine the residue functions of P, P', and ρ. These parameters are then used to fit the KN data to obtain the residue function of ω. The polarizations of the KN scatterings for which data are still lacking are predicted by the model. In connection with the speculation that the P' trajectory may behave like the ρ trajectory, three alternative trajectories are assumed for P', and their corresponding residue functions determined by the given data. The results are plotted, and we find that the "predicted" polarizations are not very sensitive to the variation of the P' trajectory. Our results show that the nonflip residue functions of both ω and ρ cross the t axis near $0<|t|<0.1$ (GeV/c)^2, while those of P and P' do not. We have established the relative sign between different trajectories. We would also like to point out that in the fittings more constraints derived from the sum rules are verified in the present work.

I. INTRODUCTION

THE presently available data on pion-nucleon scattering for incident momenta ranging from 6 to 18 GeV/c for small momentum transfer $[|t|<1$(GeV/c)$^2]$ are analyzed by a model characterized by the dominance of several meson Regge poles in the crossed channel. [The units of t are (GeV/c)^2 and the units of $d\sigma/dt$ are mb (GeV/c)$^{-2}$; they will be omitted from here on.] Several constraints in the form of simple sum rules from the model are tested in the fit. By assuming several possible trajectories for the P' pole, the data are exhaustively studied to evaluate various alternative residue functions. We first check to see that the Regge-pole model is indeed in good agreement with the known experimental data of π^+p and π^-p elastic scattering and the charge-exchange reactions $\pi^-p\to\pi^0n$ and $\pi^-p\to\eta^0n$. We also analyze the KN reactions, including K^-p, K^-n, K^+p, K^+n elastic scattering and the $K^-p\to\bar{K}^0n$ charge-exchange reactions, with the meson trajectories P, P', ρ, A_2, and ω as the contributing Regge poles.

The principal results of this work are: (a) The charge-exchange scattering of $\pi^-p\to\pi^0n$, as well as the elastic π^+p and π^-p scattering, has definite Regge behavior near the forward angles [see Eq. (15) and Fig. 1]. (b) Instead of assuming one trajectory for the P' pole as in Ref. 1, we assume both a curved and a straight trajectory for the P' pole in fitting the $\pi^\pm p$ data, and the results are reported in Fig. 2. (c) From the present data on π^-p and π^+p elastic scattering, we plot in Fig. 3 the curves of the difference of these cross sections, $d\sigma/dt\times(\pi^-p)-d\sigma/dt(\pi^+p)$, for several energies, and they all show a characteristically similar behavior, namely, they go to zero around $t\simeq-0.1$, become large but negative around $t\simeq-0.15$, and then tend gradually toward a small negative value around $t\simeq-0.9$. When we take this into account in fitting the data, the flip and nonflip residue functions for ρ are obtained and presented in Fig. 4. They are somewhat different from those of Ref. 1. (d) $\pi^\pm p$ elastic polarizations are studied with this model. Their fits determine the flip and nonflip residue functions of P, P' and ρ. (e) The ω trajectory is in-

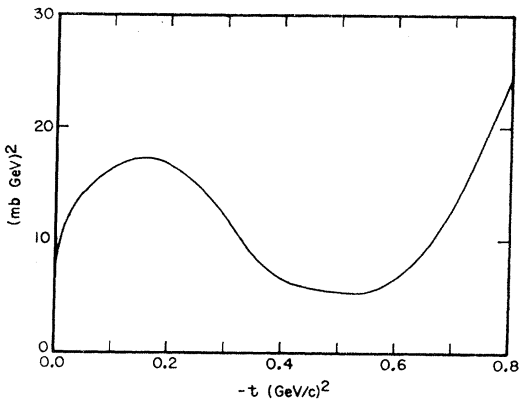

FIG. 1. Value of $f_\rho^2(t)+[f_\rho'(t)\alpha_\rho(t)]^2$ as defined in Eq. (15), plotted versus $-t$. These values are obtained by fitting Eq. (15) to the data from Ref. 11.

* Work supported in part by the U. S. Atomic Energy Commission.

[1] C. B. Chiu, R. J. N. Phillips, and W. Rarita, Phys. Rev. 153, B1485 (1967).

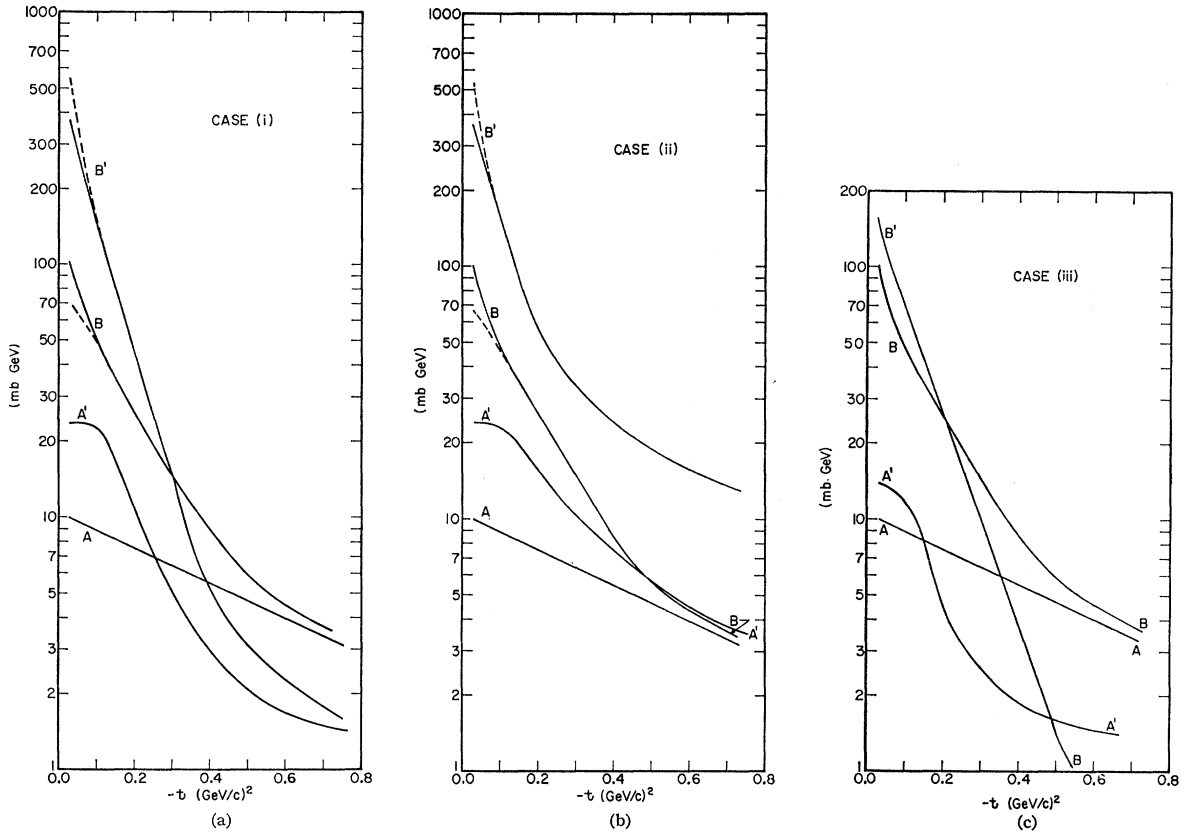

FIG. 2. Residue functions of P and P' trajectories. They are obtained from fitting Eq. (9) to the data in Ref. 13. The residues for the P trajectory are denoted by $A(t)$ and $B(t)$, and those for the P' trajectory by $A'(t)$ and $B'(t)$. The three cases are explained in the text The fits are not unique, especially for $|t|>0.5$.

vestigated by fitting the KN data. We will see that the residues of ω and ρ behave rather similarly, with their nonflip residue functions crossing the t axis around $0<|t|<0.1$ and becoming negative for large momentum transfer. (f) KN elastic and inelastic scatterings are fitted, and their polarizations are reported. (g) Relative signs between the different residue functions are established.

In Sec. II, relevant formulas necessary for the fitting are given. In Sec. III, fits to the πN cross-section data and elastic polarizations are reported. In Sec. IV, KN elastic-scattering data as well as some inelastic KN scatterings events are studied.

II. FORMALISM

In the Regge-pole model, formulas describing pion-nucleon and kaon-nucleon scattering and further descriptions of the model are easily found in the literature.[2,3] Three quantities that are useful to our later discussion are the total cross section

$$\sigma_T(s)=\mathrm{Im}A(s,\ t=0)/p\,, \tag{1a}$$

the differential cross section

$$\frac{d\sigma}{dt}(s,t)=\frac{1}{\pi s}\left(\frac{M_N}{4k}\right)^2\left[\left(1-\frac{t}{4M_N{}^2}\right)|A|^2+\frac{t}{4M_N{}^2}\left(s-\frac{s+p_\pi{}^2}{1-(t/4M_N{}^2)}\right)|B|^2\right], \tag{1b}$$

and the polarization

$$P(s,t)=\frac{-\sin\theta_s\ \mathrm{Im}(AB^*)}{16\pi s^{1/2}d\sigma/dt}\,, \tag{1c}$$

where s is the square of the c.m. energy, p is the pion laboratory momentum, k is the pion c.m. momentum, and $P(s,t)$ is the polarization defined relative to the direction of $\mathbf{p}_{\mathrm{in}}\times\mathbf{p}_{\mathrm{out}}$.[4]

The meson Regge poles contributing to the πN scatterings are P, P', ρ, and A_2 trajectories. Each trajectory will contribute to the helicity-nonflip and helicity-flip

[2] R. J. N. Phillips and W. Rarita, Phys. Rev. **139**, B1336 (1965).
[3] V. Singh, Phys. Rev. **129**, 1889 (1963).
[4] R. J. N. Phillips, Lectures given at Erice Summer School, 1966 (unpublished).

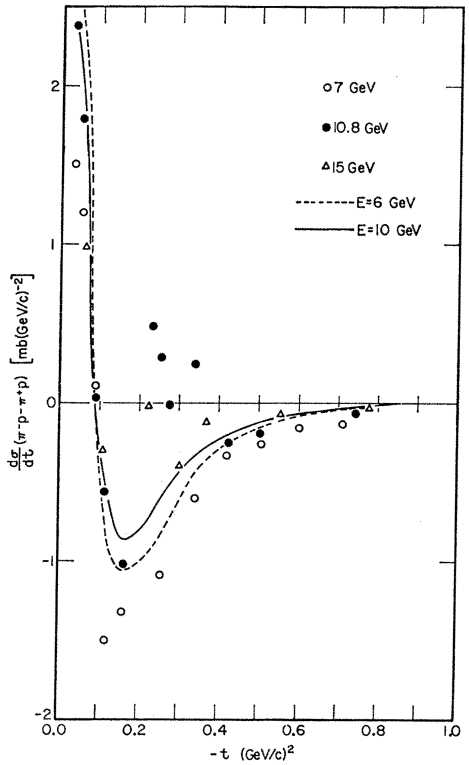

FIG. 3. Difference of $\pi^- p$ and $\pi^+ p$ differential cross sections plotted versus $-t$. We plot the measurements at three energies: 7, 10.8, and 15 GeV. The solid curve is the curve calculated from the values in Figs. 2 and 4. The different cases (i), (ii), and (iii) make little difference in the solid curve, for P always dominates P'.

amplitudes in the following manner:

$$A_i = -\frac{\bar{A}_i(t)[e^{-i\pi\alpha_i} \pm 1]}{\sin(\pi\alpha_i)}\left(\frac{E}{E_0}\right)^{\alpha_i}, \qquad (2a)$$

$$B_i = -\frac{\bar{B}_i(t)[e^{-i\pi\alpha_i} \pm 1]}{\sin(\pi\alpha_i)}\left(\frac{E}{E_0}\right)^{\alpha_i - 1}, \qquad (2b)$$

where $\bar{A}_i(t)$, $\bar{B}_i(t)$ are the reduced residue functions, and α_i is the trajectory of the contributing meson. E_0 is a scale parameter, and is taken to be 1 GeV. E is the total pion laboratory energy. The $\pm$ signs are the well-known signatures, $+$ for P and P' and $-$ for ρ and ω.

In this work, we shall adopt the following trajectories for P and ρ poles[5]:

$$\alpha_P(t) = -1 + \frac{[1+\alpha_P(0)]^2}{1+\alpha_P(0)-\alpha_P'(0)t},$$

$$\alpha_\rho(t) = 0.55 + 0.89t,$$

with $\alpha_P(0)=1$ and $\alpha_P'(0)=0.34$.

[5] The trajectory is a two-parameter form suggested by A. Pignotti [Phys. Rev. Letters **10**, 416 (1963)] which includes some curvature. While for the ρ trajectory we adopt the commonly accepted form of a straight line, it vanishes at $t=-0.6$ [see the discussion by C. Chiu Phys. Rev. **147**, B1045 (1966)]. $\alpha_\rho(t=0.0)=0.55$ was determined also by the author in Ref. 7 by using the data on the difference between the $\pi^- p$ and $\pi^+ p$ total cross sections.

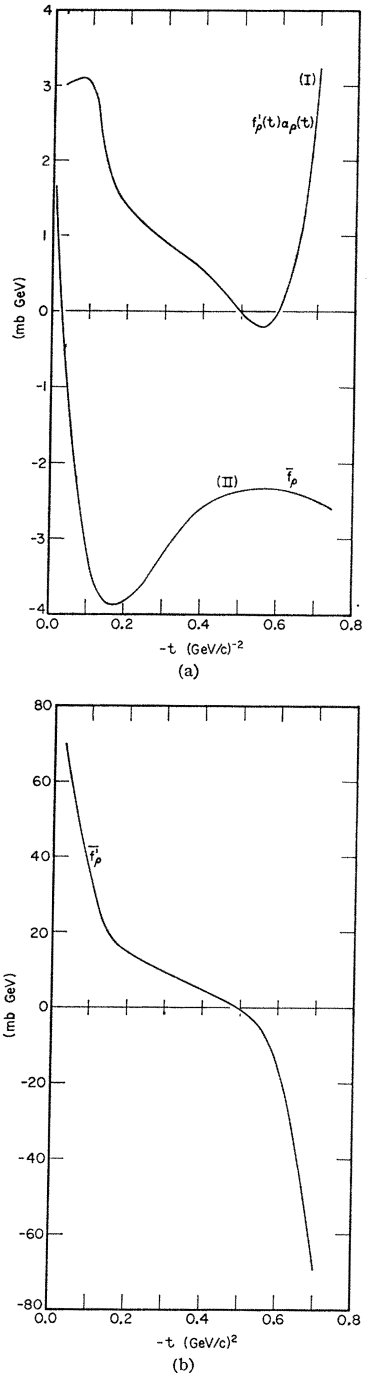

FIG. 4. (a) Residue functions of the ρ plotted versus $-t$. They are obtained by fitting to Eq. (10). We see that $f_\rho^2(t)+[f'(t)\alpha_\rho(t)]^2$ is equal to the value in Fig. 1, where $\bar{f}_\rho=(1-t/4M_N^2)^{-1/2}f_\rho$. (b) The same curve as I in Fig. 4(a), scaled to get the new residue function

$$\bar{f}_\rho' = f_\rho'(t) \Big/ \left(\frac{|t|}{4M_N^2}\frac{1}{(1-t/4M_N^2)}\right)^{1/2}.$$

The reduced residue functions can be obtained from this by using Eq. (14).

$\alpha_P(0)=1$, $\alpha_P'(0)=0.34$ were taken from Ref. 2; they are in good agreement with our investigation.

The helicity-nonflip amplitudes for the π^-p and the π^+p elastic scattering have contributions only from P, P', and ρ trajectories.

$$A(\pi^-p\to\pi^-p)=A_P+A_{P'}+A_\rho, \tag{3}$$

$$A(\pi^+p\to\pi^+p)=A_P+A_{P'}-A_\rho. \tag{4}$$

For the πp and Kp charge exchange reactions, only ρ and A_2 contribute, so that

$$A(\pi^-p\to\pi^0n)=-\sqrt{2}A_\rho, \tag{5}$$

$$A(\pi^-p\to\eta^0n)=A_{A_2}, \tag{6}$$

$$A(K^-p\to\bar{K}^0n)=2A_\rho(K)+2A_{A_2}(K), \tag{7}$$

$$A(K^+n\to K^0p)=-2A_\rho(K)+2A_{A_2}(K). \tag{8}$$

Note that we use (K) to indicate the amplitudes connected with KN scattering; they are different from the πN amplitudes.

In order to study the behavior of the above amplitudes, we shall make use of several constraint relations. They are simple sum rules contained in Eqs. (3)–(8). That we stress these sum rules in the fitting is one of the main features of this work as compared Ref. 1. From the available data, each constraint is able to provide a relation from which the behavior of residue functions of P, P', or ρ can be more completely derived. Subsequently, we are able to draw the conclusion that the theoretical differential cross sections for forward scattering in $\pi^\pm p\to\pi^\pm p$ and $\pi^-p\to\pi^0n$, at $0<|t|<1$, are in good accord with this multiple-Regge-pole model. The first relation is obtained from Eqs. (3)–(5):

$$\frac{1}{2}\left[\frac{d\sigma}{dt}(\pi^-p)+\frac{d\sigma}{dt}(\pi^+p)-\frac{d\sigma}{dt}(\pi^-p-\pi^0n)\right]$$
$$=\frac{1}{\pi s}\left(\frac{M_N}{4k}\right)^2\left[\left(1-\frac{t}{4M_N^2}\right)|A_P+A_{P'}|^2+\frac{t}{4M_N^2}\left(s-\frac{s+p_\pi^2}{1-t/4_NM^2}\right)|B_P+B_{P'}|^2\right], \tag{9}$$

where the right-hand side is independent of the ρ parameters. The experimental data available for the left-hand side range from $E=6$ to 18 GeV/c and will provide the information for the combined residue-function behavior of $P+P'$ with varying $|t|$.

Another constraint relation, deduced from Eqs. (3) and (4), is

$$\frac{d\sigma}{dt}(\pi^-p)-\frac{d\sigma}{dt}(\pi^+p)=\frac{4}{\pi s}\left(\frac{M_N}{4k}\right)^2$$
$$\times\left[\left(1-\frac{t}{4M_N^2}\right)\mathrm{Re}[A_\rho^*(A_P+A_{P'})]+\frac{t}{4M_N^2}\left(s-\frac{s+p_\pi^2}{1-t/4M_N^2}\right)\mathrm{Re}[B_\rho^*(B_P+B_{P'})]\right]. \tag{10}$$

The third relation is obtained by combining Eqs. (5)–(7).[6] It has been determined previously in Ref. 7 that ρ and A_2 are, within experimental error, members of $SU(3)$ octet (see also Ref. 4 for discussion). Hence we can use the following $SU(3)$ relations for the vertices

$$2A_\rho(K^+K^-)=A_\rho(\pi^+\pi^-),$$
$$(2\sqrt{\tfrac{2}{3}})A_{A_2}(K^+K^-)=A_{A_2}(\eta\pi).$$

These relations, together with Eqs. (5)–(7), give

$$\frac{d\sigma}{dt}(K^-p\to\bar{K}^0n)-\frac{1}{2}\frac{d\sigma}{dt}(\pi^-p\to\pi^0n)$$
$$-\frac{3}{2}\frac{d\sigma}{dt}(\pi^-p\to\eta^0n)=(2\sqrt{\tfrac{3}{2}})\left(\frac{1}{\pi s}\right)\left(\frac{M_N}{4k}\right)^2$$
$$\times\left[\left(1-\frac{t}{4M_N^2}\right)\mathrm{Re}[A_\rho^*(\pi)A_{A_2}(\eta\pi)]+\frac{t}{4M_N^2}\left(s-\frac{s+p_\pi^2}{1-t/4M_N^2}\right)\mathrm{Re}[B_\rho^*(\pi)B_{A_2}(\eta\pi)]\right]. \tag{11}$$

The reason for using Eq. (7) instead of (8) is that presently no experimental data for $K^+n\to K^0p$ are available.

Equations (9)–(11) will serve as a guide to determine the ρ, P, and P' residue functions, especially their sign changes with respect to variation of t and the relative signs among them.

In the Sec. III, the fit to the data will be presented. Since the form of the P' trajectory as well as that of A_2 is still uncertain, we will assume three alternative forms for P':

$$\text{(i)}\quad \alpha_{P'}(t)=-1+\frac{[1+\alpha(0)]^2}{1+\alpha(0)-\alpha'(0)t}=-1+\frac{(1.+0.5)^2}{1+0.5-0.34t}, \tag{12a}$$

$$\text{(ii)}\quad \alpha_{P'}(t)=0.5+0.85t \text{ so that}^8\ \alpha_{P'}(-0.6)=0, \tag{12b}$$

$$\text{(iii)}\quad \alpha_{P'}(t)=-1+(1.7)^2/(1+0.7-0.34t), \tag{12c}$$
$$\alpha_{A_2}(t)=-1+[1+\alpha_{A_2}(0)]^2/[1+\alpha_{A_2}(0)-\alpha_{A_2}'(0)t],$$

with

$$\alpha_{A_2}(0)=0.35,\quad \alpha_{A_2}'(0)=0.44, \tag{12d}$$

where in (iii) $\alpha_{P'}(0)=0.7$ is taken instead of 0.5. For

[6] The additional information obtained from the difference between the π^-p and π^+p diffraction peaks was also obtained by G. Höhler *et al.*, Z. Physik **181**, 293 (1964). See also R. K. Logan Phys. Rev. Letters **14**, 921 (1965); and Ref. 2.

[7] F. S. Chen-Cheung, Phys. Rev. **156**, B1520 (1967).

[8] S. C. Frautschi, Phys. Rev. Letters **17**, 722 (1966). All the related information about the degenerate trajectory can be found there.

each alternative assumed, the fitted residue functions and polarizations are plotted in Fig. 2. More detailed discussion of this will be presented in Sec. III.

III. FITTING THE DATA AND CALCULATION OF $\pi^{\pm}p$ ELASTIC POLARIZATION

Most of the fits to the data are obtained by hand computation, since we do not postulate any explicit expression for the residue functions. All the fits are within experimental errors. The uncertainties in the parameters obtained are not more than 1%.

The general behavior of the residue functions is still unknown, so instead of postulating an explicit form for them, we shall start with the simplest forms as follows[9,10]:

$$\begin{aligned}
&\bar{A}_P(t)=A(t)\alpha_P(\alpha_P+1),\\
&\bar{B}_P(t)=B(t)\alpha_P(\alpha_P+1),\\
&\bar{A}_{P'}(t)=A'(t)\alpha_{P'}(\alpha_{P'}+1),\\
&\bar{B}_{P'}(t)=B'(t)\alpha_{P'}(\alpha_{P'}+1),\\
&\bar{A}_\rho(t)=f_\rho(t)(\alpha_\rho(t)+1)/(1-t/4M^2{}_N)^{1/2},\\
&\bar{B}_\rho(t)=f_\rho'(t)\alpha_\rho(t)\\
&\qquad\times[\alpha_\rho(t)+1]\Big/\left(\frac{|t|}{4M_N{}^2}\frac{1}{(1-t/4M_N{}^2)}\right)^{1/2},
\end{aligned}\tag{13,14}$$

where $\bar{A}_P$, $\bar{B}_P$, $\bar{A}_{P'}$, $\bar{B}_{P'}$, $\bar{A}_\rho$, and $\bar{B}_\rho$ are the reduced residue functions defined in Eq. (12).

We now list the procedures of our fitting:

(a) Residue functions for the ρ pole can be determined by Eq. (1b) and the data of Stirling *et al.*[11] For this purpose, it is more convenient to reexpress Eq. (1b) as[12]

$$\frac{d\sigma}{dt}=\frac{2}{\pi s}\left(\frac{M_N}{4k}\right)^2[f_\rho{}^2(t)+f_\rho{}^2(t)\alpha_\rho{}^2(t)][\alpha_\rho(t)+1]^2\times\left[1+\left(\frac{\cos(\pi\alpha_\rho)-1}{\sin(\pi\alpha_\rho)}\right)^2\right]E^{2\alpha_\rho}.\tag{15}$$

Instead of postulating explicit forms[10] for $f_\rho(t)$ and $f_\rho'(t)$, we can examine the over-all behavior of the data by rewriting Eq. (15).

$$\frac{d\sigma}{dt}(\pi^-p\to\pi^0n)\Big/\frac{2}{\pi s}\left(\frac{M_N}{4k}\right)^2(\alpha_\rho+1)^2\times\left[1+\left(\frac{\cos(\pi\alpha_\rho)-1}{\sin(\pi\alpha_\rho)}\right)^2\right]E^{2\alpha_\rho}=f_\rho{}^2(t)+[f_\rho'(t)\alpha_\rho]^2.\tag{16}$$

For each fixed t, we compute the left-hand side of Eq. (16) for $E=5.9$, 9.8, 13.3, and 18.2 GeV (where $d\sigma/dt$ are the data from Ref. 11). Note that these four computed quantities (at a given t) are quite close to each other. Within experimental error, they can be taken to be equal to each other up to $t=-0.5$. This energy independence is in fact required by the right-hand side of Eq. (16), and hence[10] it can be said that the Regge behavior is well satisfied by the data of $\pi^-p\to\pi^0n$ in Ref. 11 up to $t=-0.5$. For larger values of t, the data at 18.2 GeV give values slightly different from those given by other three energy values. Hence for $|t|$ larger than 0.5, we take the values determined from these three energies, and they gave fairly consistent results. Finally, we plot the value of $[f_\rho{}^2(t)+f_\rho'{}^2(t)\alpha_\rho{}^2]$ versus t in Fig. 1. The curve in Fig. 1 does not determine $f_\rho(t)$ and $f_\rho'(t)$ separately. However, the $f_\rho(0)$ value is fixed by total-cross-section data and takes the value of 1.62, or, equivalently, the reduced residue at $t=0$ is $\bar{A}_\rho(0)=2.5$.

(b) Next, we study the P and the P' poles, using Eqs. (9) and (13) and the data in Ref. 13. We find that in general the data can be fitted well. $A(t)$, $B(t)$, $A'(t)$, and $B'(t)$ as defined in Eq. (13) decrease as $|t|$ increases. At $t=0$, the data[14] for $\sigma_{\rm tot}(\pi^-p)+\sigma_{\rm tot}(\pi^+p)$ give the reduced residue functions at this point as $\bar{A}(0)=20$ mb GeV, $\bar{A}'(0)=18$ mb GeV. Again, for fixed t, data on the the left-hand side of Eq. (9) give energy-independent values for the residue function at several energies. This, together with the polarization data in Ref. 15, enables one to determine completely the residue functions $A(t)$, $B(t)$, $A'(t)$, and $B'(t)$, which are plotted in Fig. 2. Cases (i), (ii), and (iii) correspond to the alternative forms assumed for the P' trajectory.

(c) The relative sign of the ρ and P residue functions can be determined. Equation (10), together with data from Refs. 13 and 14, can be used for this purpose. Only at the incident momentum of 10.8 GeV/c were measurements made for both π^+p and π^-p at exactly the same laboratory energy. At the other energies the incident momenta are slightly different for π^+p and π^-p (e.g.,

---

[9] We are only interested in obtaining the reduced residue functions, so we have arbitrarily assumed the factor of $\alpha(\alpha+1)$ in them. However, one may reexpress them in any useful form one prefers (for example, with explicit kinematic factors, etc.). This factor is different from the one in Ref. 1, but the conclusion we draw about $A(t)$, $B(t)$, $A'(t)$, and $(B't)$ (see text) will not be changed if we use the same factor.

[10] After this paper was written we were informed that a similar conclusion has also been reached by G. Höhler *et al.*, Phys. Letters **20**, 79 (1966). They also treated the residue functions without parametrizing.

[11] A. V. Stirling *et al.*, Phys. Rev. Letters **14**, 763 (1965).

[12] The second factor in Eq. (1b) can be written as

$$\frac{-t}{4M_N{}^2}\frac{st/4M_N{}^2+p^2}{1-t/4M_N{}^2}=\frac{-t}{4M_N{}^2}\left(\frac{p^2}{1-t/4M_N{}^2}\right);$$

this gives about 6% error when $E=6$ GeV and $t=-0.7$, but the error is much smaller when E becomes large and $t\to 0$. This expression is fitted to the over-all behavior of the data first, and then we refit the data, using the exact expressions.

[13] K. J. Foley *et al.*, Phys. Rev. Letters **11**, 425 (1963).

[14] W. Galbraith *et al.*, in *Proceedings of the Twelfth Annual International Conference on High-Energy Physics, Dubna, 1964* (Atomizdat, Moscow, 1965). The ρ parameters at $t=0$ will be fixed uniquely by taking $\sigma_{\rm tot}(\pi^-p)-\sigma_{\rm tot}(\pi^+p)$ (see Ref. 7).

[15] M. Borghini *et al.*, Phys. Letters **21**, 115 (1966).

TABLE I. A_2 parameters for $\pi^- p \to \eta^0 n$, including the trajectory parameters of the A_2 [Eq. (17)] and the residue-function parameters as given in Ref. 7.

$\alpha(0)$	$\alpha'(0)$	C_0	C_1	D_0	D_1
0.35	0.44	5	1.7	−95	2.6

8.8 and 8.9 GeV/c, respectively), but we shall still make use of them. We present these data for the left-hand side of Eq. (10) in Fig. 3. We observe that the difference of the differential cross section $d\sigma/dt(\pi^- p) - d\sigma/dt(\pi^+ p)$ crosses the t axis at $t \simeq -0.1$, and takes on a large negative value of the order -1 mb at around $0.1 < |t| < 0.2$. It then approaches a small negative value of about -0.02 m bat $t = -0.8$. The oscillatory behavior in the interval of $0.2 < |t| < 0.4$ is neglected. Using the values of $A(t)$, $B(t)$, $A'(t)$, and $B'(t)$ in Fig. 2, this curve in Fig. 3 now determines $f_\rho(t)$ and $f_\rho'(t)\gamma_\rho(t)$. The results are plotted in Fig. 4, and we note that they satisfy the constraint given by Fig. 1. We also note that in Eq. (10) the contribution of the P trajectory dominates that of the P' trajectory, so that the three alternative cases in Fig. 2 give about the same effect in computing Eq. (10).

At small values of t, around $t = -0.03$, we found that the relative sign of $B(t)$ and $f_\rho'(t)$ must be positive in order to obtain the large positive values of $d\sigma/dt(\pi^- p - \pi^+ p) = 3.5$ for $E = 10.8$, while $f_\rho(t)$ is also positive relative to $A(t)$ but changes sign around $t = -0.03$. At this value of $t = -0.03$, the values[16] of A, B, A', B', $f_\rho(t)$, and $f_\rho'(t)\alpha_\rho$ are still uncertain, for the polarization data are still not available at this point. New experimental data at this point would be valuable (the polarization data in Ref. 15 start at $t = -0.1$). In conclusion, we obtain $f_\rho(t)$ and $f_\rho'(t)\alpha_\rho(t)$ as plotted in Fig. 4. The result is similar to that in Ref. 1, but we believe that the residue function may not be expressible by simple equations like the ones given in Ref. 1. We also note that the spin-flip residue function $f_\rho'(t)$ changes sign at around $t = -0.5$, for this seems to give a better fit to Eq. (11) with the present data. If $f_\rho'(t)$ remains positive, then a positive value is obtained for $t = -0.7$ in Eq. (11), instead of a negative value as given by the data. However, the data are still too uncertain for one to say any more than this.

(d) Relative sign of the ρ and A_2 residue functions: Equation (11) will be used for this purpose. We assume a curved trajectory for A_2,

$$\alpha_{A_2} = -1 + \frac{[1+\alpha_{A_2}(0)]^2}{1+\alpha_{A_2}(0) - \alpha_{A_2}'(0)t} = -1 + \frac{(1.35)^2}{1.35 - 0.44t} \quad (17)$$

and solution 1 from Ref. 7 is used, which we list for convenience in Table I. Using the results of the ρ residue function as given in Fig. 4, we obtain the fit to Eq. (11) and present the result in Table II. We find that the reduced residue $\bar{A}_{A_2}$ is positive and $\bar{B}_{A_2}$ is negative, which is in agreement with the result listed in Ref. 7.

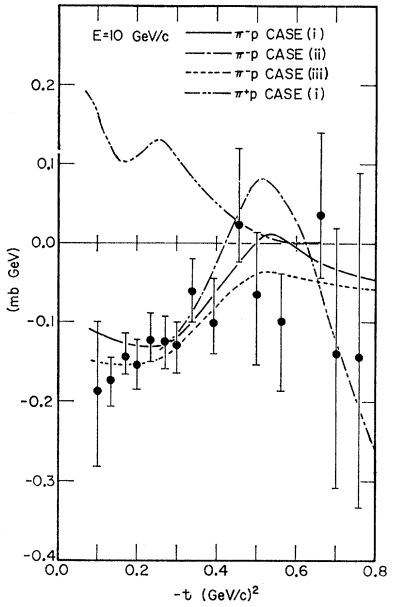

FIG. 5. Fit of the $\pi^- p$ polarization for $E = 10$ GeV in Ref. 15. The theoretical value is indicated by the solid curve. We note that for $|t| > 0.5$, the data are uncertain, but that a fit to more accurate data could easily be made.

[16] The residue functions $A(t)$, $A'(t)$, $B(t)$, and $B'(t)$ are not necessarily straight when plotted on semilogarithmic paper, but in the forward direction, i.e., at small t, they are well approximated by a straight line, which indicates an exponentially decreasing function of $|t|$. We shall leave them the way they are in Fig. 2. for this work.

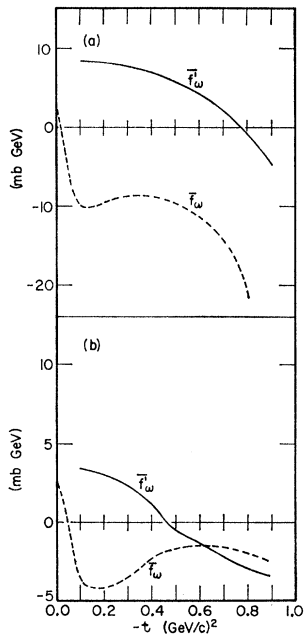

FIG. 6. ω residue functions. We use Eqs. 27 and 28 for (a) and (b), respectively.

$$\bar{f}_\omega = (1 - t/4M_N^2)^{1/2} f_\omega, \bar{f}_\omega' = f_\omega' \Big/ \left(\frac{|t|}{4M_N^2} \frac{1}{(1 - t/4M_N^2)}\right)^{1/2}.$$

TABLE II. Comparison of Eq. (11) with the experimental values and the theoretical computations.

t	−0.02	−0.05	−0.07	−0.17	−0.27	−0.37	−0.5	−0.6	−0.7
Experimental points given by the left-hand side of Eq. (11) (μb)	$3\pm\epsilon$	$36\pm\epsilon$	$47\pm\epsilon$	$100\pm\epsilon$	$60\pm\epsilon$	$30\pm\epsilon$	$-3\pm\epsilon$	$-3.4\pm\epsilon$	$-5.1\pm\epsilon$
Calculated value of the right-hand side of Eq. (11)[a] (μb)	9	20	49	32	22	10	−1	−3.6	−2

[a] Here ϵ, the uncertainty of the experimental data, is very large, especially for $\pi^-p\to\eta^0n$; therefore we shall view the fitting in this table only as a tool to check the relative signs of the flip and nonflip amplitudes of the mesons involved (A_2, ρ).

There is speculation[8] that A_2 and ρ may be completely degenerate and can be described by one trajectory. However, from the fit to the πN total-cross-section data[4] we found that $\alpha_{A_2}(0)=0.35$, while $\alpha_\rho(0)=0.55$. To further test this hypothesis, A_2 was made degenerate with ρ and the over-all behavior of the data for the reaction[17] $\pi p\to\eta n$ were studied. We found that the complete degeneracy hypothesis is a poor assumption. Instead, we take Eq. (11d) as the trajectory for A_2. This is a curved trajectory, and its extrapolation to $t=+1.7$ will give the right mass[3] for the A_2. However, the data can also be fairly well fitted by taking $\alpha_{A_2}(t)=0.34+0.58t$.

Using the residue functions for the P, P', and ρ poles which can be read off Figs. 2 and 4, the π^-p polarization is computed for the three alternative P' trajectories, and in Fig. 5 they are compared with the experimental points. We note that changing the sign of $f_\rho'(t)$ for the ρ pole will give a negative polarization at $t=-0.7$ if we use these residue functions. However, the residue functions can be adjusted so that they will give a negative polarization even if $f_\rho'(t)$ does not change sign. More accurate measurements of the polarization are required.

In summary, we conclude that our analysis is similar to that of Ref. 1 except that (a) we study the effect of different alternative trajectories for the P', and we also use the relations given by Eqs. (9)–(11) extensively in our analysis; (b) our ρ residue function is somewhat different from theirs, if the fit in Fig. 3 is taken seriously: (c) $f_\rho'(t)$ may change sign; (d) if the π^-p polarization is proved to have oscillatory behavior, we can still adjust the ρ residue functions to fit the data. We believe that the ρ residue function $f(t)$ may be oscillating. Better data are required to confirm this point.

Accurate measurements of $d\sigma/dt(\pi^-p)$, $d\sigma/dt(\pi^+p)$, and the π^-p polarization at $|t|>0.6$. are needed. Since the present data for $\pi p\to\eta n$ are too crude, better measurements here will also be valuable.

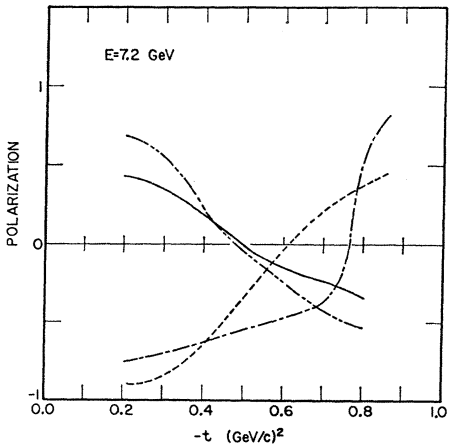

FIG. 7. Predictions of $K^\pm p$ polarizations, using Eq. (27) for ——K^+p and —·—K^-p, and Eq. (28) for —··—K^+p and ·····K^-p.

[17] O. Guisan *et al.*, Phys. Letters **18**, 200 (1965).

IV. INVESTIGATION OF SOME ELASTIC AND INELASTIC KN SCATTERINGS

The expressions for total and differential cross sections for KN scatterings are similar to that for πN scatterings in Eqs. (1) and (2). The various amplitudes to be studied are

$$A(K^-p\to K^-p)=A_P+A_{P'}+A_\omega+A_\rho+A_{A_2}, \quad (18)$$

$$A(K^-n\to K^-n)=A_P+A_{P'}+A_\omega-A_\rho-A_{A_2}, \quad (19)$$

$$A(K^+p\to K^+p)=A_P+A_{P'}-A_\omega-A_\rho+A_{A_2}, \quad (20)$$

$$A(K^+n\to K^+n)=A_P+A_{P'}-A_\omega+A_\rho-A_{A_2}, \quad (21)$$

$$A(K^-p\to\bar{K}^0n)=2A_\rho+2A_{A_2}, \quad (22)$$

$$A(K^+n\to K^0p)=-2A_\rho+2A_{A_2}, \quad (23a)$$

where all the amplitudes A_i are the amplitudes with respect to KN scattering. The relations between Kn and πN amplitudes are as follows:

$$\begin{aligned} A_P(\pi N)&=A_P(KN),\\ A_\rho(\pi N)&=2A_\rho(KN),\\ A_{A_2}(\pi N)&=(2\sqrt{\tfrac{2}{3}})A_{A_2}(KN). \end{aligned} \quad (23b)$$

The relations for the P' and ω trajectories are unclear presently. In this work we find, for the P' pole, that its contribution to KN scattering is about 10% of that to πN scattering.

We notice that the ω trajectory has come into play now, but its nature is still little known. However, we can determine $\alpha_\omega(0)$ and its reduced nonflip residue function at $t=0$ from the data on the total cross section[14]

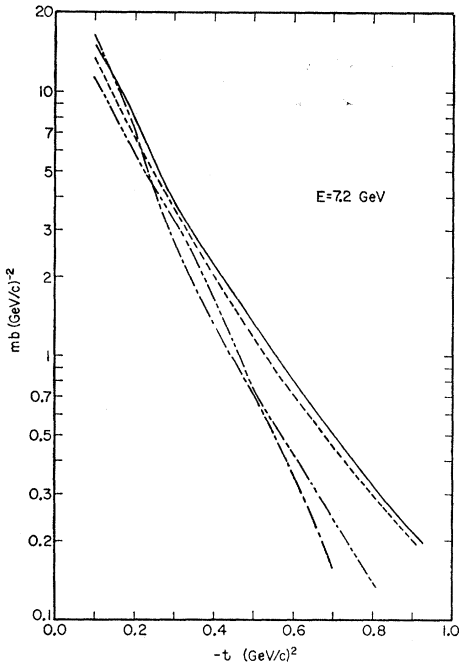

FIG. 8. Predictions for $K^{\pm}n$ differential cross sections, using Eq. (27) for ——K^+n and —·—K^-n, and Eq. (28) for ·····K^+n and —··—K^-n.

for KN scattering. From Ref. 14, we have

$$\sigma_{\rm tot}(s)(K^-p+K^-n)=2\ {\rm Im}(A_P+A_{P'}+A_\omega)/p, \quad (24)$$

$$\sigma_{\rm tot}(s)(K^+p+K^+n)=2\ {\rm Im}(A_P+A_{P'}-A_\omega)/p, \quad (25)$$

and from these equations

$$\sigma_{\rm tot}(K^-p+K^-n)-\sigma_{\rm tot}(K^+p+K^+n) =4\ {\rm Im}A_\omega(t=0)/p. \quad (26)$$

Now if we express as usual the spin-flip and spin-nonflip terms as follows:

$$A_\omega=-f_\omega(\alpha_\omega+1)\left(\frac{e^{-i\pi\alpha_\omega}-1}{\sin\pi\alpha_\omega}\right)E^{\alpha_\omega},$$

$$B_\omega=-f_\omega'\alpha_\omega(\alpha_\omega+1)\left(\frac{e^{-i\pi\alpha_\omega}-1}{\sin\pi\alpha_\omega}\right)E^{\alpha_\omega-1},$$

then the data will provide us $\alpha_\omega(0)$ and $A_\omega(0)$ through Eq. (26)[18]:

$$\alpha_\omega(0)=0.7,$$
$$A_\omega(0)=4.4.$$

If we reinsert these values into Eq. (24), we can estimate that the contribution of P' to KN here is only about 10% of that to πN. In the following we shall take this as a working assumption. We shall take two alternative forms for the ω trajectory:

$$\text{(a)}\quad \alpha_\omega(t)=0.7+1.17t, \quad (27)$$

so that $\alpha_\omega(0.6)\simeq 0$;

$$\text{(b)}\quad \alpha_\omega(t)=-1+(1.7)^2/(1.7-0.14t), \quad (28)$$

so that the extrapolation of t to the mass of ω will give $\alpha_\omega\simeq 1$.

Now to extract the information on the ω residue functions, we fit the data on K^+p and K^-p elastic scattering in Ref. 19:

$$\frac{d\sigma}{dt}(K^-p+K^+p)=\frac{1}{\pi s}\left(\frac{M_N}{4k}\right)^2 \times\left[2\left(1-\frac{t}{4M^2_N}\right)\left[\left|A_P+A_{P'}+\frac{A_{A_2}}{2\sqrt{\frac{2}{3}}}\right|^2 +|A_\omega{}^k+\tfrac{1}{2}A_\rho|^2+\frac{2t}{4M^2_N}\left(s-\frac{s+p^2}{1-t/4M^2_N}\right) \times\left(\left|B_P+B_{P'}+\frac{B_{A_2}}{2\sqrt{\frac{2}{3}}}\right|^2+|B_\omega{}^k+\tfrac{1}{2}B_\rho|^2\right)\right]\right], \quad (29)$$

where we have converted the relevant quantities from the πN amplitudes by means of the $SU(3)$ relations in Eq. (23a), except for $A_\omega{}^k$ and $B_\omega{}^k$, where k indicates the KN amplitude.

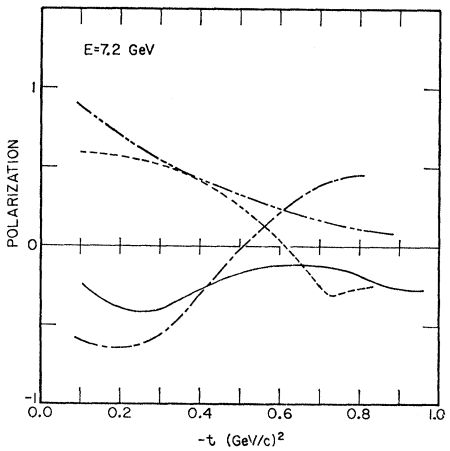

FIG. 9. Predictions for $K^{\pm}n$ polarization, using Eq. (27) for —··—K^+n and ——K^-n, and Eq. (28) for ·····K^+n and —·—K^-n.

[18] Here the ω pole will stand for both ω and ϕ, which belong to the same octet as ρ but partly also to a singlet. The recent article of V. Flores-Maldonado, Phys. Rev. **155**, B1773 (1967) gives $\alpha_\omega(0)=0.5$, which is smaller than the value we obtained from fitting to the total-cross-section data. However, there is no well-established value for this quantity, so we shall continue to use the one we obtained in this paper, $\alpha_\omega(0)=0.7$.

[19] K. J. Foley *et al.*, Phys. Rev. Letters **11**, 503 (1963).

Using the results obtained in the above sections for P, P', ρ, and A_2, taking case (i) for P', we obtain the residue functions of ω as plotted in Fig. 6. We then proceed to present the predictions for the K^+p and K^-p polarizations in Fig. 7. Finally, the predictions for K^-n and K^+n elastic differential cross sections are given in Fig. 8, and their polarizations in Fig. 9. The above calculations are based on the contribution of the Regge poles from the t channel alone.

ACKNOWLEDGMENTS

We would like to thank Dr. F. Cheung, Dr. E. Golowich, Dr. H. Feier, Dr. J. Belinfante, Dr. G. Renninger, and Dr. B. Deo for their interest and helpful discussions. We are indebted to Professor R. E. Cutkosky for his encouragement and helpful discussions. We also wish to thank Professor C. Meltzer for many helpful discussions.

PHYSICAL REVIEW VOLUME 173, NUMBER 5 25 SEPTEMBER 1968

Parameters of Low-Energy Λ-K^0 Production

J. EDWIN RUSH, JR.
University of Alabama in Huntsville, Huntsville, Alabama 35807
(Received 16 May 1968)

A pole-resonance model is used to fit the data for $\pi^-p \to \Lambda K^0$ from threshold to 1200 MeV. Parameters of the three pole contributions are taken from a study of the 1370–2200-MeV region, with form factors employed. The reduced widths of eight resonances are then determined by minimizing χ^2. The most significant contributions to the process are found to be those of the $P_{11}(1470)$ and $S_{11}(1710)$, although other resonances are also important. The results are discussed with consideration given to $SU(3)$ assignments and parity doubling.

1. INTRODUCTION

DESPITE the theoretical work of many authors on the process $\pi^-p \to \Lambda K^0$ over a period of several years, one cannot say that the following objectives have been realized: a clear understanding of the contributions of poles and resonances to the low-energy region, and a reliable determination of the pole and resonance parameters. These parameters are important for the assignment of $SU(3)$ multiplets and the determination of D/F ratios of octets, for evaluation of the predictions of symmetry schemes in addition to those of $SU(3)$, and in general for assessing the validity of any dynamical theory of the strong interactions. The present existence of a large collection of experimental data, both differential cross sections and polarization angular distributions, together with the results of recent phase-shift analyses, would seem to eliminate the principal obstacles to achieving the aforementioned objectives. It is our purpose in this paper to present a determination of the low-energy ΛK^0 parameters by fitting the data with pole and resonance contributions. In view of the complexity of the isospin-$\frac{1}{2}$ spectrum of baryon resonances, we can conceive of no reliable way to determine these parameters other than an analysis of the partial-wave amplitudes similar to that given here.

A discussion of most of the earlier models was included in a previous paper[1] and will not be repeated here. However, a relatively recent paper dealing with the low-energy region, which is not mentioned in Ref. 1, is that of Hoffman and Schnitzer.[2] These authors used the Cini-Fubini approximation to the Mandelstam representation to study the region near threshold. The only "well-established" $I=\frac{1}{2}$ resonances at that time were the F_{15} and the D_{13}, and they approximated the latter by a real amplitude. Thus the only imaginary amplitude resulted from the F_{15}, and other important contributions, notably that of the imaginary part of the $S_{11}(1710)$, were not included. This probably accounted for their failure to obtain a good fit to the polarization data.

In this paper, we present a study of the energy region from threshold (768 MeV) to 1200 MeV which was done by varying pole and resonance parameters to fit the data. In order to take account of all three Mandelstam channels, we used poles due to the nucleon, the Σ, and the $K^*(890)$. Resonances which were included are the well-known[3] $S_{11}(1550)$, $S_{11}(1710)$, $P_{11}(1470)$, $D_{13}(1525)$, $D_{15}(1680)$, and $F_{15}(1690)$, as well as two new resonances predicted recently by Donnachie *et al.*,[4] a $P_{11}(1751)$ and a $P_{13}(1863)$. The pole parameters were first studied by using the pole terms alone in a simple model at higher energies,[5] where one-particle exchange should begin to

[1] J. E. Rush and W. G. Holladay, Phys. Rev. **148**, 1444 (1966).

[2] H. Hoffman and H. J. Schnitzer, Nucl. Phys. **76**, 481 (1966).

[3] For references to data on these states, see A. H. Rosenfeld, N. Barash-Schmidt, A. Barbaro-Galtieri, L. R. Price, P. Söding, C. G. Wohl, M. Roos, and W. J. Willis, Rev. Mod. Phys. **40**, 77 (1968).

[4] A. Donnachie, R. Kirsopp, and C. Lovelace, Phys. Letters **26B**, 161 (1968).

[5] The higher-energy data used are at eight energies 1.4–2.2 GeV, recently published by O. I. Dahl, L. M. Hardy, R. I. Hess, J. Kirz, D. H. Miller, and J. A. Schwartz, Phys. Rev. **163**, 1430 (1967).